UPPSALA
UNIVERSITET

UPTEC F 23038
Examensarbete 30 hp
Juni 2023

LoRa Based Moisture Sensing System

Rasha Badran

Civilingenjörsprogrammet i teknisk fysik

UPPSALA UNIVERSITET

LoRa Based Moisture Sensing System

Rasha Badran

Abstract

Water is an important parameter for crop growth, and the information about the moisture content in soil at different depths is very useful for farmers to determine the best time to water the soil and to irrigate farmland so as to maximize their yield.

This thesis project aims to develop a prototype of a multi-depth moisture sensor probe that is part of a large sensing system used in agriculture. The sensor probe has three sets and is required to last for 6-12 months of usage and to be reproduced at a low cost.

The sensor probe consists of three sensor boards, on each of which has two different capacitive based sensors and one analog temperature sensor. The three boards are placed approximately 20 cm from each other in the probe. During this project, the two capacitive based sensors were developed, one with arc-shaped plates operating at a frequency less than 1 MHz, and one with electrodes in the form of annular rings operating at a high frequency, approximately 100 MHz. The moisture content in the soil is calculated based on the measurement of the frequency, which depends on the dielectric constant of the soil.

For the implementation of the sensor probe, three printed circuit boards (PCBs) for the sensor boards were designed using Altium Designer and then ordered; an STM32 Nucleo board with low power microcontroller was used and the software was implemented in STM32CubeIDE. The lifetime of the sensor probe was calculated for different duty-cycles. With a duty-cycle of 15 minutes, where the sensor probe is active for 1 minute and in sleep mode for 14 minutes, the lifetime of the sensor probe would only be 16 days. With a duty-cycle of 120 minutes instead, with the sensor probe being active for 1 minute, the lifetime is increased to 130 days (less than 4,5 months).

Due to challenges with the high frequency capacitive sensor, the multi-depth sensor probe does not fully work, and thus cannot be tested with a large testbed. Further work needs to be conducted on the high frequency capacitive sensor and the communication with the gateway.

Teknisk-naturvetenskapliga fakulteten

Uppsala universitet, Utgivningsort Uppsala

Handledare: Kjell Brunberg Ämnesgranskare: Ping Wu

Examinator: Tomas Nyberg

Populärvetenskaplig sammanfattning

Det blir allt vanligare att smarta IoT-lösningar används inom jordbruket, där man till exempel gräver ner sensorer i odlingsmarken för att mäta så väl fukthalten som temperaturen i jorden. Sensorerna genererar realtidsdata som kan användas för att optimera grödornas tillväxt. Med kontinuerliga mätningar kan det avgöras huruvida mer eller mindre bevattning krävs. För att övervaka stora odlingar krävs ett sensornätverk av sensorrör som kommunicerar med en eller flera gateway(s), som i sin tur skickar över data till en databas där mätningarna kan presenteras för bönderna. LoRaWAN-tekniken är en trådlös digital dataöverföringsteknik som ofta används då den har låg energiförbrukning och möjliggör dataöverföring över långa sträckor.

Detta examensarbete utfördes i samarbete med Swecin AB med önskan att utveckla ett batteridrivet sensorrör med sensorer på tre olika nivåer i röret, som ska kunna vara mellan 6-12 månader och som ska vara reproducerbart till en låg kostnad. I projektet ingick utvecklingen av två kapacitiva sensorer som användes tillsammans med en analog temperatursensor, kretskortsdesign samt implementation av mjukvara. Det framtagna sensorröret är en första prototyp och vidareutveckling krävs innan sensorröret kan industrialiseras.

Sensorröret består av tre kretskort med tre olika sensorer, två kapacitiva sensorer som mäter fukthalten i marken och en temperatursensor. Kretskorten har designats i Altium Designer och har placerats cirka 20 cm ifrån varandra i röret för att möjliggöra mätningar på olika djup i marken. Under projektet utvecklades de två kapacitiva sensorerna, en med halvcylindriska elektroder som mäter en frekvens på cirka 1 MHz i luft och en högfrekvenssensor med två ringar som elektroder, som mäter en frekvens på cirka 100 MHz i luft. Genom att mäta frekvensen kan omgivningens dielektriska konstant räknas fram och utifrån dielektriska konstanten kan fukthalten i sin tur räknas fram. Härledningen av ekvationerna för de två sensorernas kapacitans ingår inte i detta projekt, utan frekvensmätningarna sparas för vidare analyser.

En STM32 Nucleo board med en mikrokontroller med låg effekt användes och mjukvaran implementerades i STM32CudeIDE. Sensorrörets livslängd beräknades baserad på olika arbetscykler, för att undersöka hur ofta mätningar kan göras och samtidigt ha en så lång livslängd som möjligt. Med en arbetscykel på 15 minuter, där sensorröret är aktivt i en minut och i vila i 14 minuter är sensorrörets livslängd cirka 16 dagar. Med en arbetscykel på 120 minuter istället, där sensorerna är aktiva i en minut och i vila resten av tiden, är livslängden strax under 4.5 månader. Den aktiva tiden är satt till en minut i detta projekt, men kan undersökas vidare för att effektivisera mätningarna och förlänga sensorrörets livslängd.

Målet var dels att utveckla sensorröret och implementera mjukvaran och dels att sedan testa flera sensorrör i ett större sammanhang där sensorrören även ska kommunicera med en eller flera gateways. På grund av utmaningar med den högfrekventa kapacitiva sensorn blev projektet inte färdigt i tid och kommunikationen med gatewayen implementerades därför inte. Det fanns heller inte möjlighet att testa flera sensorrör. Endast ett sensorrör implementerades och testades under detta projekt.

Contents

Acronyms

CMOS Complementary Metal Oxide Semiconductor

ECL Emitter-Coupled Logic

HFC High Frequency Capacitance

IC Integrated Circuit

IDE Integrated Development Environment

IoT Internet of Things

LoRa Long Range

LoRaWAN Long Range Wide Area Network

LPWAN Low Power Wide Area Network

PCB Printed Circuit Board

RF Radio Frequency

VCO Voltage Controlled Oscillator

Chapter 1

Introduction

1.1 Background

In agricultural production, water is the most important requirement for crop growth [**1**]. Different weather conditions provide random impacts on crop growth. Therefore, farmers need to carefully compensate with water to be able to maximize crop growth and yield. Knowing the soil moisture content, the farmers can know when to irrigate their crops. To be able to improve harvest yield, it is important to measure soil profile moisture content accurately in real-time.

With today's larger fields, smart moisture sensing systems are becoming more popular in agriculture since they give farmers information about the humidity and temperature at different levels in the soil in real-time. The information helps the farmers to keep the optimum content of water around the crops [**1**]. The larger the fields, the more sensor probes are needed, and the higher the costs. It is therefore important to offer farmers low-cost alternatives that last longer periods.

1.2 Purpose and Goals

The goal of this thesis project is to design, implement and test a multi-depth sensor probe with real time wireless network, that can withstand and survive the real application challenges of an all-year around installation in Swedish soil. The multi-depth probe will include a high frequency fringing field moisture sensor at three different levels, approximately 20 cm apart. Each high frequency moisture sensor will also be supplemented with a capacitive sensor, a temperature sensor and low power software so that the batteries can last for 6-12 months. The thesis aims to industrialize the sensor probe so that it is reproducible at a low cost.

1.3 Tasks and Scope

The multi-depth sensor probe is part of a wireless sensing network for agriculture, where the network will monitor moisture and temperature at different levels in soil. The sensor probes in the network will be connected with low power Long Range (LoRa) radio to an internet based online presentation system, where measured parameters are presented to the farmer who will then decide what actions need to be undertaken. The radio antenna should be mechanically rugged to survive and withstand most of the mechanical and manual tools and machinery that may appear around the probe placement. To find such antenna is out of the scope of this project.

To achieve a multi-depth moisture sensor probe that can be industrialized, the following tasks need to be completed:

- Design of capacitive sensor with arc-shaped plates.
- Design of high frequency capacitive sensor with annular electrodes.
- Full design of a sensor probe with electronics and Printed Circuit Board (PCB) design.
- Software implemented to make measurement readings.
- Installation and testing of multiple sensor probes on a large test bed.

1.4 Outline

The report is organized as following. The background and motivation for this thesis are presented in **Chapter 1**, together with the tasks and scope. **Chapter 2** gives a theoretical background to capacitive sensors, capacitive-based moisture sensors and LoRa communication. **Chapter 3** presents the hardware and software used in this project, as well as the design procedure and the complete solution. Measurement results from the multi-depth sensor and discussions are presented in **Chapter 4**. **Chapter 5** finally presents conclusions based on the results and future work needed to industrialize the sensor probe.

Chapter 2

Theoretical Background

This chapter aims to describe the theoretical background of the main parts of the thesis project - the capacitive-based moisture sensors and the LoRa communication. Section 2.1.1 covers the basics of capacitive-based moisture sensors, whereas section 2.1.2 and 2.1.3 describe the sensors used in this project in more detail. Section 2.2 covers LoRa communication and the LoRa network.

2.1 Capacitive-Based Moisture Sensors

2.1.1 Basic Structure

A capacitor consists of three parts - a positive plate, a negative plate and a dielectric medium. The dielectric has a constant which indicates the material's capability to transmit electricity [**2**]. Most capacitors contain at least two electrical conductors, but the physical shapes and forms of different capacitors can vary widely, depending on the application. A basic parallel plate capacitor is shown in Fig. 2.1. The capacitance of a parallel plate capacitor can be calculated in the following manner,

$$C = \epsilon_0 \epsilon_r \frac{A}{d}, \tag{2.1}$$

where ϵ_0 is the permittivity of free space being equal to $8.854 \cdot 10^{-12} F/m$, and ϵ_r is the relative permittivity for the dielectric medium. A is the area of one of the plates in square meters and d is the separation distance between the two plates given in meter.

A capacitive-based moisture sensor features no exposed plating and uses capacitive sensing to detect soil moisture [**3**]. The sensor utilizes the electrical property of capacitance and the electrical field created around the sensor. The plates of the capacitor

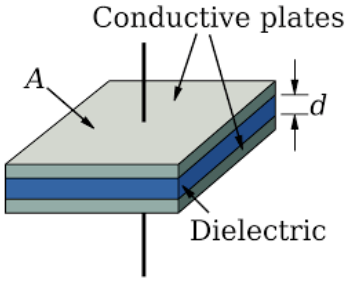

Figure 2.1: The structure of a basic parallel plate capacitor, consisting of two conductive plates and a dielectric medium in-between. A is the area of a plate and d is the separation distance between the two plates.

together with the surrounding material, the dielectric, act as a capacitor, which then generates an electrical field when voltage is applied across the plates. When the surrounding varies, it affects the stray field capacitance, and the dielectric constant of the material can then be calculated.

When using a capacitive moisture sensor, the estimated water content of the surrounding soil is based on the dielectric constant of the soil. As the water content of the soil increases, the dielectric constant of the soil increases, because the dielectric constant of water is much larger than the other soil components, including air [**4**]. Therefore, the measurement of the dielectric constant gives a predictable assessment of water content and moisture.

The capacitance can change quickly, which is an advantage, but the change is often very small, measured in pF, which makes it difficult to measure it accurately. The capacitor is therefore included in an LC-oscillator resonance tank circuit where the frequency depends on the size of the capacitance, which can be describe in the following manner,

$$f = \frac{1}{2\pi\sqrt{LC}}, \tag{2.2}$$

where f is the frequency, L is the inductance and C is the capacitance. Eq. (2.2) shows that if either L or C decreases, the frequency increases. If L or C increases instead, f decreases. This output frequency is commonly called the resonant frequency. Since C changes depending on the dielectric material between the plates, the measured output frequency changes. The signal-amplitude is constant, while the measured capacitance value is proportional to the circuit's frequency. When the frequency is measured, the capacitance can be solved from Eq. (2.2) and the constant

of the dielectric can be calculated from the capacitance.

Because of their simplicity, relatively low cost, and high accuracy, capacitive sensors have been applied to characterize the dielectric properties of many different materials [**5**]. Two types of capacitive sensors are used in this thesis, one with arc-shaped cylindrical electrodes and one with annular ring electrodes, both described further in section 2.1.2 and 2.1.3 respectively.

2.1.2 Arc-Shaped Cylindrical Electrodes

The first sensor used in this thesis is a traditional capacitive sensor with an equivalent capacitance that consists of two arc-shaped metallic plates that are located interior to and coaxially with a cylindrical tube, as shown in Fig. 2.2. The edges of the metallic plates are separated from each other with a small distance d. Since the tube has a small radius, 23 mm, and the plates are relatively short compared to the complete tube, the separation distance d does not affect the capacitance and the resonant frequency, as long at it is a couple of millimeters wide.

Figure 2.2: The cylindrical arc-shaped electrodes partially inserted in a tube, with the edges of the plates being separated with a distance d m from each other.

One of the plates is connected to signal, while the other plate is connected to ground, constituting a capacitor with the surrounding being the dielectric. Since the plates are arc-shaped, the distance between the plates vary, where the distance between the plates is larger at the center of the plates compared to the distance between the edges of the plates. The formula for this kind of capacitor is different from and more

complicated than Eq. (2.1), which is the formula for the parallel plate capacitor with a constant separation distance, but the derivation is out of the scope of this thesis project.

The resonant frequency depends on the capacitance, which in turn depends on the area of the plates. For a given radius of the arc, the longer the plates, the higher the capacitance. When the plates are shorter, with the same size of radius, the capacitance instead decreases, which gives a higher frequency. With the known formula for this kind of capacitor with arc-shaped plates, the dielectric constant of the surrounding can be calculated and the moisture content can in turn be assessed.

2.1.3 Annular Ring Electrodes

The second capacitive sensor used in this thesis follows the principle of High Frequency Capacitance (HFC) method. Two annular metal rings with width W at a distance D from each other acting as electrodes, together with the soil content, constitute an equivalent capacitor. The physical structure of this equivalent capacitor is shown in Fig. 2.3 and the formula for this kind of capacitor can be derived from Eq. 2.1), but it is out of the scope of this project. When the two rings are connected to a tank circuit and there is a voltage applied across the electrodes, they radiate an electric field around the equivalent capacitor. This field does not only exist directly between the two electrodes, but extends some distance away, which is illustrated in Fig. 2.3 as dashed lines between the electrodes. This is known as a fringing field [**6**].

Using the HFC method, the soil moisture is obtained by measuring the frequency of the tank circuit. With the known frequency, the equivalent capacitance of the soil mix of soil particles, water, etc., that serves as the dielectric between the annular electrodes [**7**] can be calculated. The dielectric constant of water is much higher than soil's and air's, and the influence of soil texture on the dielectric constant is therefore negligible at very high frequencies, at around 100-500 MHz [**7**]. Consequently, the capacitance is essentially determined by the soil moisture content.

The capacitance is measured by placing the equivalent capacitance in an oscillating LC-circuit and measuring the final frequency. The frequency depends on the equivalent capacitance, which in turn changes when the dielectric varies with e.g. moisture content. Like the case with the arc-shaped cylindrical electrodes mentioned in chapter 2.1.2, derivation of the formula for the capacitance is out of the scope of this thesis project. With the formula known, the dielectric constant of the soil can be calculated and the moisture content can be assessed.

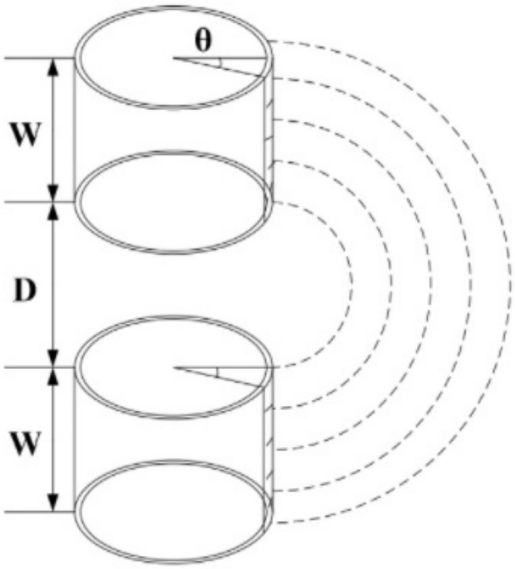

Figure 2.3: The physical structure of the annular electrodes. W is the width of the electrode and D is the axial distance between the two identical electrodes. The dashed lines represent the electrical field between the two electrodes. Image credit: [**7**].

2.2 LoRa Communication

LoRa, short term for Long Range, is a radio modulation technology enabling Low Power Wide Area Networks (LPWANs) [**8**]. Requiring low power allows the creation of battery-operated devices that can last for several years and LoRa has therefore become of interest in Internet of Things (IoT). LoRa provides communication up to five kilometers in urban areas, and up to 15 kilometers in rural areas [**8**]. These advantages of LoRa makes it a suitable choice in agricultural, where long-range communication between a large number of devices, with low power requirements and that collect small amounts of data, is needed.

In a typical LoRa network, there are four building stones: end-devices, gateways, a cloud-based network server service, and an application service. An illustration of a LoRa network from end to end is presented in Fig. 2.4. LoRa, being a wireless modulation, uses the air as a medium for transporting radio waves from a radio frequency (RF) transmitter in an IoT device, to a RF receiver in a gateway via LoRa, and vice

versa. There is no one-to-one relationship between LoRa-based devices and gateways in a LoRaWAN [8]. Messages that are sent to and from end devices travel through all gateways within range. The gateway then transmits the data via a standard IP connection to the network server [8], converting RF packets to IP packets and vice versa. The network server then handles data deduplication [8], among other things.

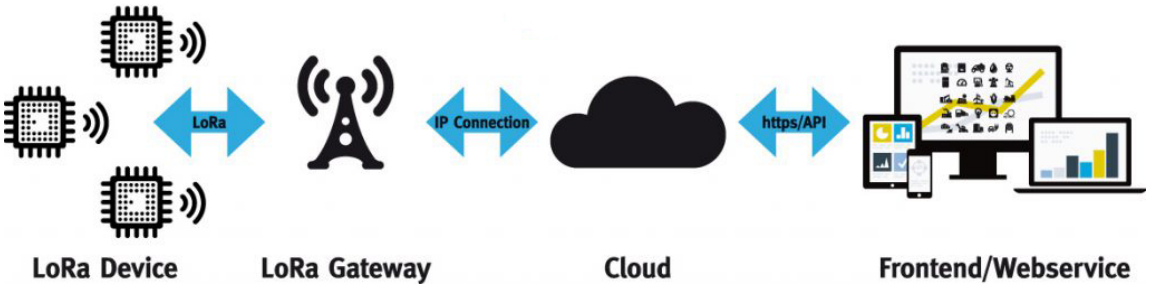

Figure 2.4: End-to-end LoRa network. Image credit: [9].

LoRaWAN is the connectionless network system architecture and communication protocol for LoRa. LoRaWAN is a Media Access Control (MAC) layer protocol that enables LoRa in wider applications. It is an open networking protocol that delivers secure bi-directional communication, mobility, and localization services standardized and maintained by the LoRa Alliance.

LoRaWAN is the communication protocol and system architecture for the network, while LoRa is the physical radio layer enabling the long-range communication link. The LoRaWAN protocol and network architecture directly influence the battery lifetime of a node, network capacity, quality of service, security, and the variety of applications served by the network.

2.2.1 Device Classes: A, B and C

There are three device classes which a LoRa-based end-device may operate in when communicating with the network - Class A, B, and C [8]. All devices must support Class A operation, which is the least power-consuming class. For a device to operate in Class B, it must support both Class A and Class B modes. A device operating in Class C mode must therefore support all three modes of operation.

In Class A mode, the end device spends most of its time in sleep mode, and the application of the end device cannot wake up the Class A device [8]. Instead, the

end device wakes up when it is configured to wake up, initiates an uplink and transmits data to the network. After that, the end device listens for a response from the network for a given time period. If no downlink is received during that period, the device goes back to sleep, waking up a moment later to listen for a response again. If no response is received during this second receiving window, the device goes back to sleep until the next time it has data to report or until it is programmed to wake up [**8**].

When a device is in sleep mode, the power consumption is very low and measured in milliwatts (mW). When data packets are transmitted, the required energy is also quite low, given that the data packets are very small and only transmitted a few times a day. This allows the batteries to last for a long period of time.

A device operating in Class B mode consumes more energy than a device operating in Class A mode since it offers regularly-scheduled, fixed-time receiving windows for the end device to receive downlinks from the network, in addition to the receiving windows that open whenever a Class A uplink is sent to the server [**8**]. For the end-device to open the receive window at the scheduled time, it receives a time-synchronized beacon from the gateway, which allows the server to know when the end-device is listening [**9**].

Class C devices are most suited when the downlink transmission is important for the application since the end device listens continuously for messages from the gateway. The end devices only close the receiving windows when they are transmitting an uplink message [**8**].

Chapter 3

Methods and Implementation

Both hardware and software are used and developed in this project and the different main hardware components needed to develop the moisture sensors, together with the software and development tools used, are presented below in sections 3.1 and 3.2 respectively.

The design procedure of the sensor probe is presented in section 3.3, where the designs of the two capacitive-based humidity sensors are described, together with the design of the complete sensor probe.

3.1 Hardware and Components

3.1.1 Microcontroller

STM32WL55 Nucleo board (Fig. 3.1) is a long-range wireless and ultra-low-power microcontroller that features RF transceiver supporting LoRa modulation [**10**]. The device is dual-core and based on the ARM Cortex-M4, complemented by an ARM Cortex-M0+ [**10**]. Both processors are for embedded systems and provide low power consumption. Cortex M0+ has the lowest power consumption in the Cortex-M family [**11**] and is the main processor used in the software implementation in this project. There are several low-power modes supported by STM32WL55 that helps achieve the best compromise between low power consumption, short startup time, available peripherals and available wake up sources [**11**]. Sleep mode is one of these low power modes which turns off the CPU of the processor to keep the power consumption very low, but keeps the peripherals running. All peripherals can stay running and wake up the CPU when an interrupt or an event occurs [**11**].

There are different versions of the STM32WL55 microcontroller, and the one used in

the first testings in this project is STM32WL55CCU7. It has 29 GPIO pins and each pin can be configured by the software as an input, output or as a peripheral alternate function [**11**]. The STM32 Nucleo board has different types of timers, among them three general purpose timers with different channels that can be used to generate PWM outputs, or act as simple time bases. The different channels for the general purpose timers are input capture, output compare, and PWM [**11**]. The input capture mode allows the user to automatically store the timer's value when an event happens on a pin. This channel comes in handy when a frequency is to be measured. As for the output compare, this channel toggles a pin whenever the value in the timer reaches a certain amount. The PWM toggles a pin at different duty cycles based on a timer's counter value.

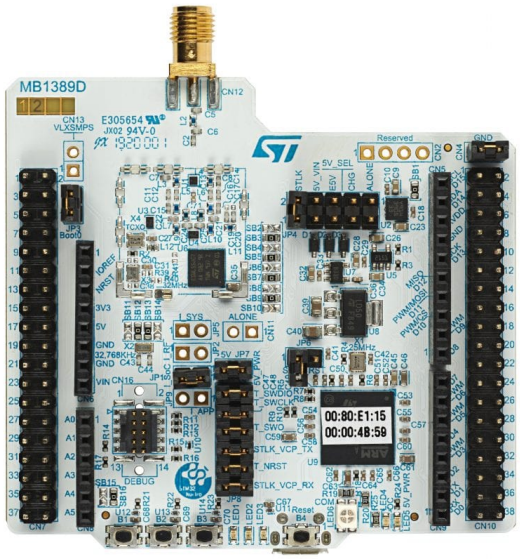

Figure 3.1: The dual-core STM32WL55 Nucleo board used in the first testings of the project.

3.1.2 555 timer

A commonly used timer is the 555 general purpose timer. It is a low cost, robust and widely used Integrated Circuit (IC) [**12**] that can be used in different applications. The well known name of the timer comes from the three serially connected 5k resistors

in the IC circuit [**12**].

There are different versions of the 555 IC timer, and the two main versions are the SE and NE versions. The only difference between these two versions is the operating temperature range [**12**], where the SE has a wider operation temperature range than the NE. There are also low power versions of the 555 timer, the Complementary Metal Oxide Semiconductor (CMOS) versions. A CMOS version is used in this project. This version offers significant performance advantages over the standard 555 timer, such as lower power consumption and virtually non-existent current spike during output transition [**13**].

All versions of the 555 timer can operate in two different modes: monostable mode and astable mode. In the monostable mode, the timer acts as a one-shot [**13**], which means that a signal is produced when the timer is triggered. The signal goes high and stays high for some time before it goes low and remains low until the circuit is triggered again [**12**]. In the astable mode the free running frequency and the duty cycle are determined by two external resistors and a capacitor. The values of the resistors and the size of the capacitor are described further in section 3.3.1.

3.1.3 Emitter-Coupled Logic Voltage Controlled Oscillator Amplifier

An oscillator whose oscillation frequency is controlled by a voltage input is called a Voltage Controlled Oscillator (VCO). By varying the input voltage, the frequency is also varied. There are different types of VCO circuits. An Emitter-Coupled Logic (ECL) VCO is one type and is the type used in this project, the MC100EL1648.

ECL is a high-speed IC bipolar transistor logic family, which is the fastest logic device family currently available [**14**]. The high speed in the ECL is achieved by it's non-saturated mode of operation. The emitter current of the transistor is limited to avoid the saturated region. High speed is also achieved because of the low RC time constants maintained in the IC by the use of smaller resistor values [**14**].

MC100EL1648 is a VCO amplifier that requires an external parallel tank circuit consisting of an inductor (L) and capacitor (C) [**15**]. Fig. 3.2 illustrates a block diagram of the device with its pins, together with the tank circuit. A test circuit with an alternating tank circuit is shown in Fig. 3.3. Instead of using a 0.1 μF capacitor in the tank circuit to the far left (between pin 8 and ground), another type of capacitor is used. More about that in section 3.3.2. This configuration generates a

varying frequency output when the capacitance of the capacitor replacing the 0.1 μF capacitor is varied.

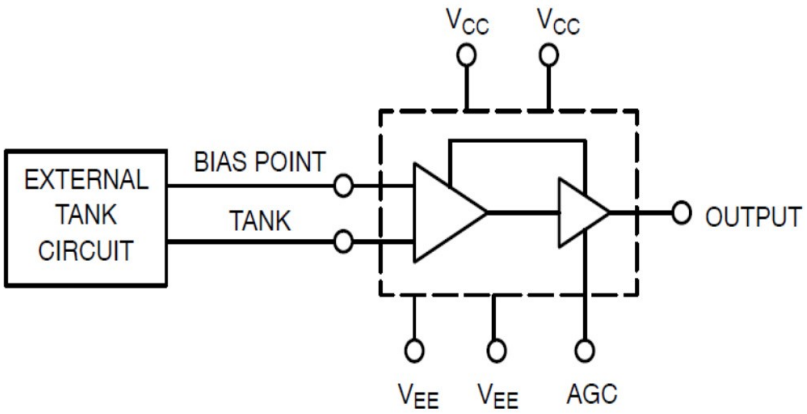

Figure 3.2: Block diagram of MC100EL1648 with the required tank circuit and the pins. V_{CC} is the positive power supply, V_{EE} is negative output, and OUTPUT is the ECL output. AGC stands for Automatic Gain Control Input. Image credit: [**15**].

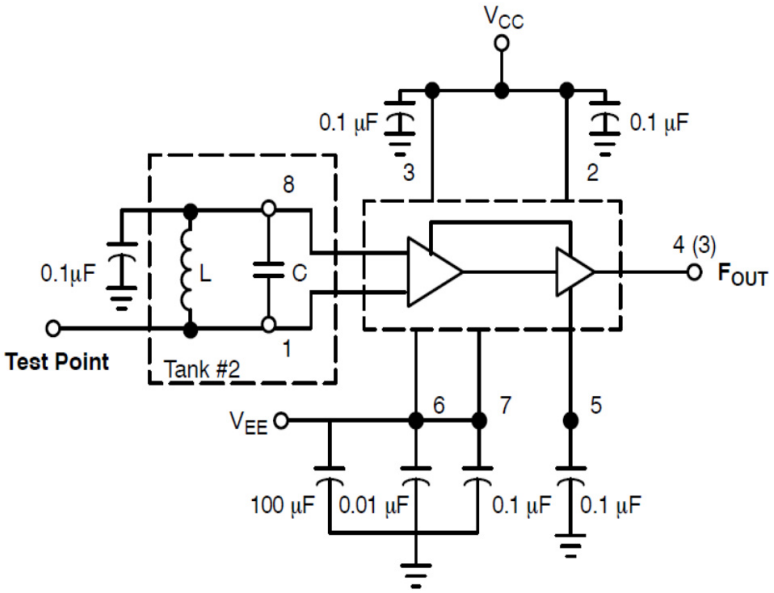

Figure 3.3: Example of a test circuit from the datasheet with alternate tank circuit. Image credit: [**15**].

3.1.4 Low Voltage Temperature Sensor

LMT85 is a precision CMOS temperature sensor with ± 0.4°C typical accuracy [**16**]. It is a low voltage temperature sensor that provides an output between -0.3 V and $V_{DD} + 0.5$ V, with V_{DD} being the power supply with a range between 1.8 V and 5.5 V. The relationship between the output voltage and the temperature is described by the parabolic Eq. (3.1) and temperatures between -50°C and 150°C can be calculated from equation (3.1) when the output voltage V_{TEMP} is measured [**16**].

$$T = \frac{8.194 - \sqrt{(-8.194)^2 + 4 \cdot 0.00262 \cdot (1324 - V_{TEMP}(mV))}}{2 \cdot (-0.00262)} + 30 \tag{3.1}$$

The analog LMT85 temperature sensor is primarily chosen for this project because of its low power operation and wide temperature range: -50°C to 150°C [**16**]. No other external components are needed for the sensor to operate. It just needs to be connected according to Fig. 3.4, where pin 1 is connected to power supply, pin 2 to the microcontroller to read the output and pin 3 to ground.

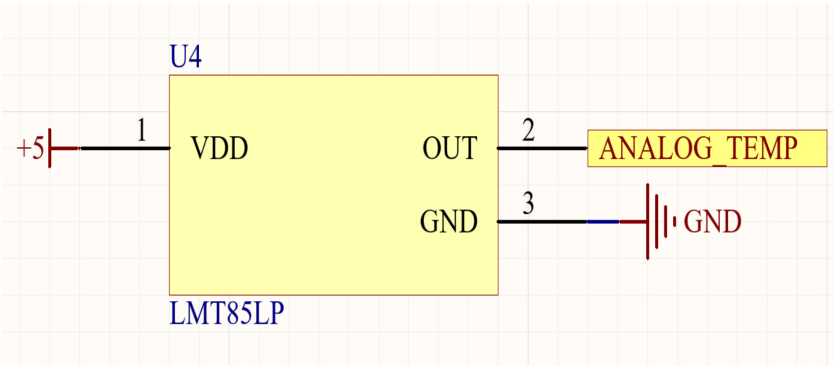

Figure 3.4: Schematic for the analog temperature sensor with three pins. One pin is for the power supply, one for the output voltage and one pin is connected to ground.

3.1.5 Multiplexer/Demultiplexer

A multiplexer, shortly called MUX, is a logic circuit which acts as a switcher when multiple inputs are connected to a single common output line. A demultiplexer, also called a DEMUX, performs the reverse operation of a multiplexer, where a single input is connected to several outputs.

The multiplexer used in this project is the CD4053B, which can be used both as a MUX and a DEMUX. It is a triple 2-channel and can deliver both analog and digital signals. CD4053B has three separate digital selector variable inputs, A, B, and C, and an inhibit input [**17**]. Fig. 3.5 shows the functional block diagram of CD4053B. Depending on the states of the selector variables, the user can control which channel to read from or write to. When A is low, logic 0, channel *ax* is on. When A is high, logic 1, *ay* is the chosen channel. It does not matter what the states of the other selector variables B and C are, only the state of A decides which *a*-channel is to be chosen. The *b*- and *c*-channels are chosen in the same way, by controlling the selector variables B and C respectively.

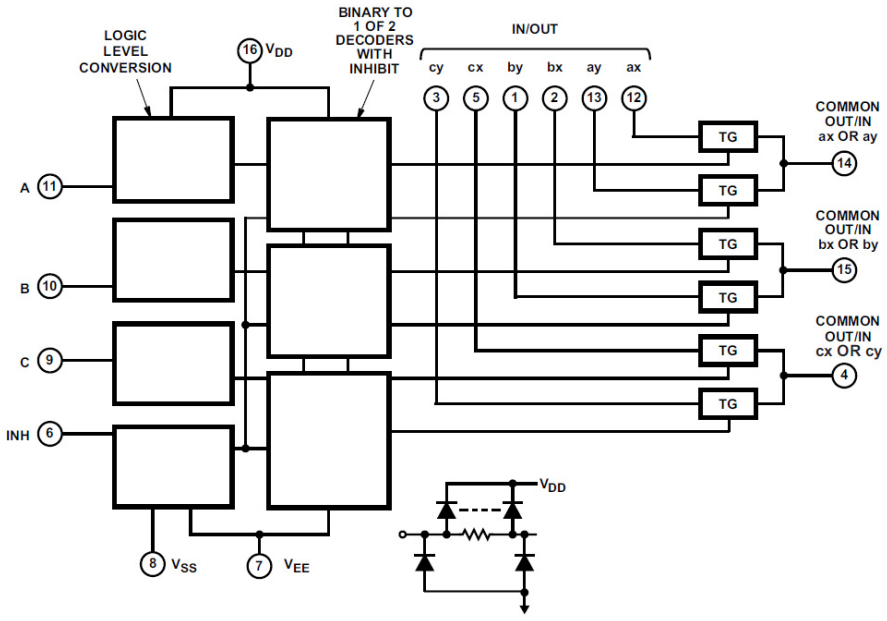

Figure 3.5: Functional block diagram of CD4053B [**17**]. The states of the selector variables A, B, and C decide which channel to read from or write to.

3.2 Software and Development Tools

3.2.0.1 Integrated Development Environment for STM32

To develop software, an Integrated Development Environment (IDE) is needed. It is a tool that provides the user interface code development, testing and debugging features [**18**]. STM has its own IDE, STM32CubeIDE, which is an advanced C/C++ development platform [**19**]. It includes peripheral configuration, code generation, as well as code compilation and debug features for STM32 microcontrollers and microprocessors [**20**].

When using STM32CubeIDE, the user chooses either an empty or a pre-configured microcontroller or microprocessor from the selection in the IDE. A project is then created and the initialization code is generated. The user can return to the initialization at any time during a project development and re-configure peripherals or middleware. The initialization code can then be regenerated without any impact on the user code [**20**].

3.2.1 Altium Designer

The design of the electronics for the sensors and the sensor board were created in Altium Designer, which is a software for electronic design and PCB design.

All electronics for the sensors are first connected in schematics. Each component needs a footprint before it can be placed out on the PCB, where the footprint is the pattern for an electronic component with the information of e.g. size, number of pins, and distance between pins, etc. Altium has a footprint wizard where many footprints for different components can be found. Sometimes, footprints for some components cannot be found in the footprint wizard, and therefore need to be created or imported. Altium offers the opportunity of creating footprints, as well as importing footprints from other sources.

In the PCB design, Altium Designer has a simple user interface and the user is offered both 2D and 3D editing modes. A PCB can be designed, shared, and sent to manufacturing all in the same software program.

3.3 Design Procedure

The LoRa based humidity sensing system consists of sensor probes, a gateway and a database. This project covers the design of the sensor probe and the communication between each probe and a gateway. The rest of the sensing system, the communication between the gateway and the database and the presentation of the data, is covered by another student's thesis project and are therefore not included in this report. The plan is to combine the two projects to have a complete sensing system network.

Each sensor probe in the sensing system consists of three different sensors (two moisture sensors and one temperature sensor) at three levels in the probe, making it a total of nine sensors. The probe used in this project is one meter long, and it is therefore approximately 20 cm between one level and the other. Each sensor in a probe must communicate with a microcontroller, which then sends the packaged data to a gateway. The gateway then sends the packaged data over to a database through IP connection. This thesis project includes the design of the two moisture sensors and the PCB design of the three sensors together. The communication between the sensors and a gateway was originally part of the project, but due to lack of time it was excluded.

The designs of the two capacitive moisture sensors are described in section 3.3.1 and 3.3.2, respectively. An analog temperature sensor is also used in this project and its circuit is presented in a previous section, section 3.1.4. The complete design of the sensor probe is then described in section 3.3.3, with the three sensors at three different levels in each probe. One probe contains a total of three PCBs, one PCB for each level. The designed PCB is also presented in section 3.3.3.

3.3.1 Capacitive Sensor with Arc-Shaped Cylindrical Electrodes

A general purpose CMOS low power version of the 555 RC timer is used to generate a free running frequency. It is configured in astable mode, where the frequency f in Eq. (3.2) is controlled by the two external resistors R_A and R_B, and the capacitance C [**13**] consisting of the two arc-shaped cylindrical metal plates.

$$f = \frac{1.46}{(R_A + 2R_B)C} \tag{3.2}$$

With the two arc-shaped plates of the capacitor C having the length 5 cm, the resistors R_A and R_B are chosen to generate a frequency at around 1 MHz in air, and are

therefore chosen to be 10 kΩ and 3.3 kΩ respectively. These values give a frequency of 1.4 MHz in air. The schematic of the capacitive sensor is shown in Fig. 3.6, where the arc-shaped plates are represented by pads P1-P8 and the output OUT_555 is connected to the microcontroller (more about the connections to the microcontroller in section 3.3.3). Only two of the pads are connected to the capacitive sensor's circuit - pad P1, to connect one plate to signal, and pad P5, to ground the other plate. The other pads are to connect the plates to the PCB for stability. The capacitance C11 in the schematic in Fig. 3.6 is chosen to give a clear output square wave signal and is chosen to be 0.01 μF. Other values of C11 give a sawtooth-like wave.

The pads that are made on the PCB for the cylindrical arc-shaped plates is shown in Fig. 3.7, on which the plates are soldered on, both for connection and stability. The plates are more stable if all four corners of the plates are soldered to the PCB. In Fig. 3.8 it can be seen how it looks like with the plates of the capacitor mounted on the PCB.

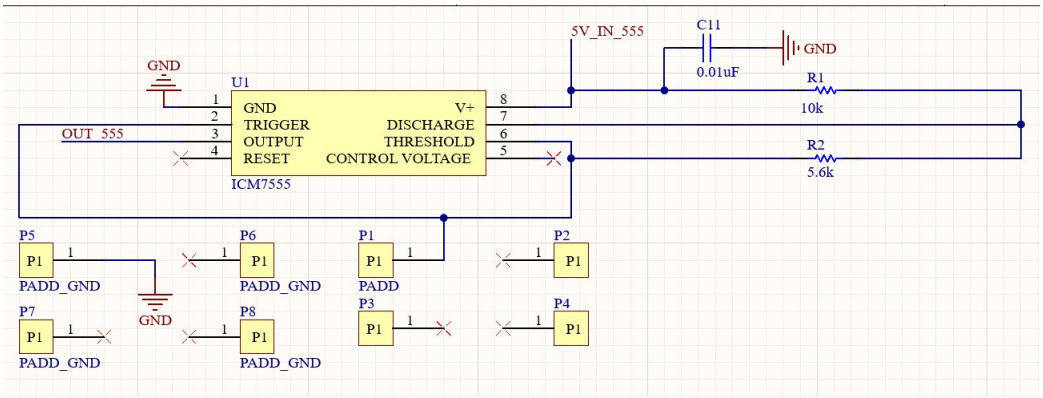

Figure 3.6: The schematic of the capacitive sensor. The 555 timer, together with the resistors R_A, R_B, the capacitor $C11$ and the pads P1-P8 for the arc-shaped plates.

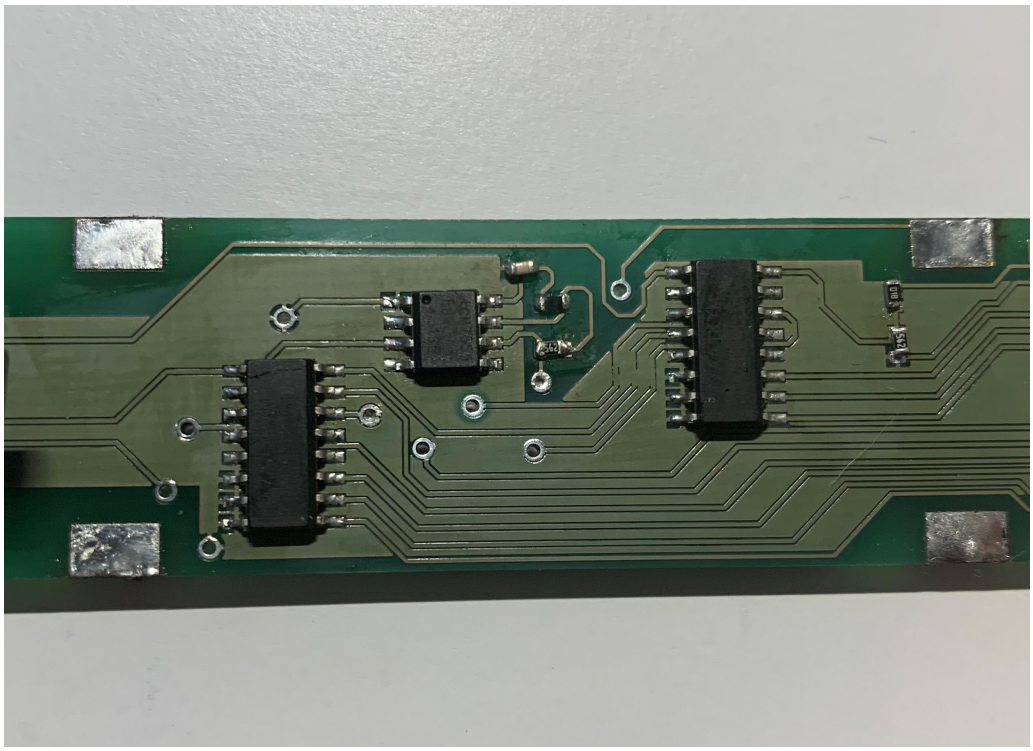

Figure 3.7: The hardware of the capacitive sensor with the components soldered onto the PCB, where the pads on the PCB can be seen in the corners of the included part of the PCB.

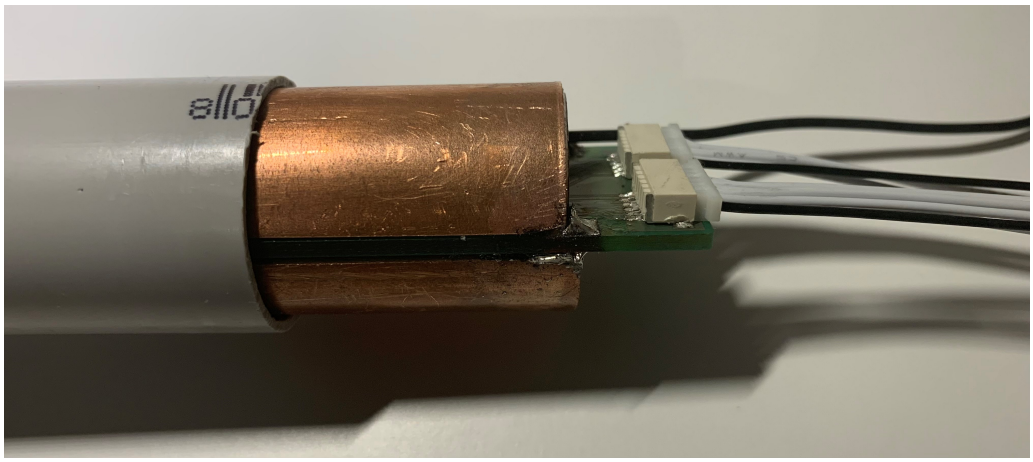

Figure 3.8: The hardware of the capacitive sensor with the two arc-shaped electrode plates mounted on the PCB, which is partially inserted into the probe.

3.3.2 High Frequency Fringing Field Sensor with Annular Ring Electrodes

For the high frequency capacitive sensor using the HFC method, an ECL VCO is used, together with an external parallel tank circuit consisting of an inductor L and some capacitors creating an equivalent capacitance C. The schematic of the VCO together with the tank circuit is presented in Fig. 3.9, where the chosen component values can be seen. The component values are chosen in a way to give an output frequency at approximately 100 MHz in air. When the two metal annular electrodes are connected to the circuit and radiating the electric field around the periphery, the measured soil and the two electrodes covered by the radiation electric field constitute an equivalent capacitor together [**7**], which is part of the equivalent capacitance C in the LC tank.

The two larger pads S1 and S2 in Fig. 3.9 are the pads for the annular metal ring electrodes. The annular rings are 10 mm wide and have the same circumference as the probe's inside, i.e. a radius of 11 mm and a circumference of 69 mm. The output OUT_VCO at pin 4, which is shown in Fig. 3.9, is first connected to a logic level converter, which in turn is connected to a frequency divider to scale down the frequency in order to be able to measure it with the microcontroller. The logic level converter is used to convert the ECL signal to a CMOS signal, since the frequency divider is a CMOS type. Fig. 3.10 shows the complete HFC sensor with the hardware and the annular rings soldered onto the PCB.

3.3.3 Complete Design

As previously mentioned, the sensor probe consists of three different sensors placed at three different levels in the probe, approximately 20 cm distance between the levels. A PCB is designed with the electronics for the three sensors, and placed at each level in the probe. Each probe therefore consists of three PCBs, one microcontroller and a power source in the form of 4x1,5V AA batteries. In section 3.3.3.1, the power source is described in more detail, before the design of one level is presented in section 3.3.3.2 and the design of the complete sensor probe with three levels is described in section 3.3.3.3.

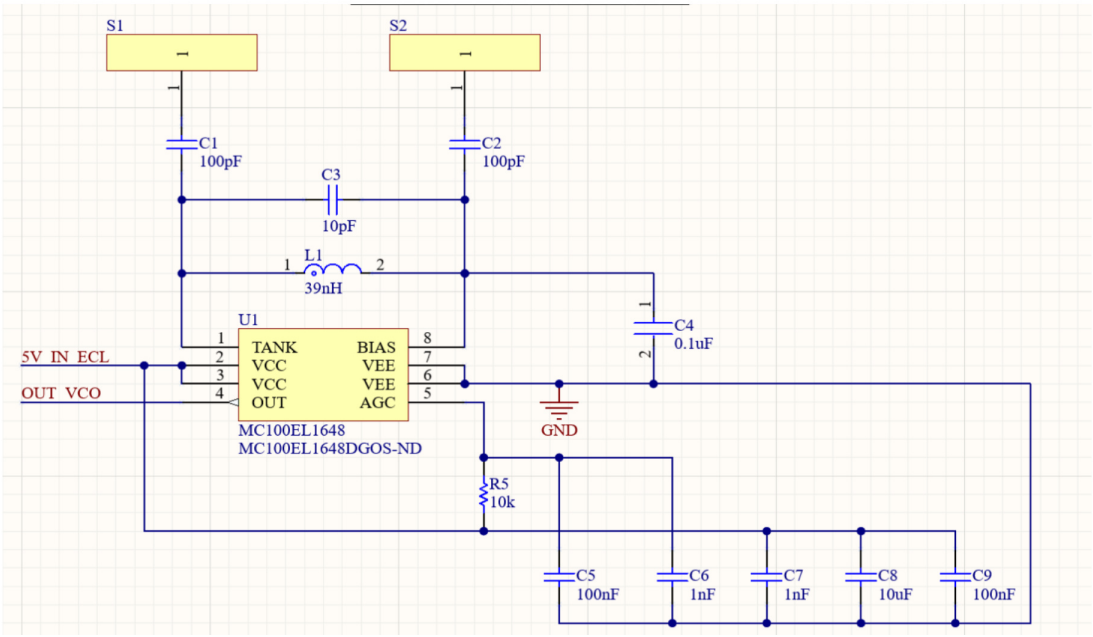

Figure 3.9: The schematic of the HFC sensor. The VCO, together with the tank circuit between pin 1 and 8, and the equivalent capacitance constituted of the two pads S1 and S2 and the surrounding environment.

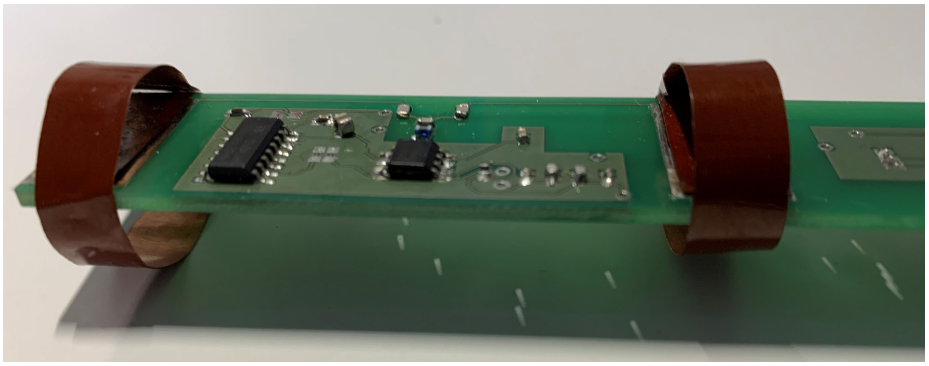

Figure 3.10: The layout of the HFC sensor, with the components and the annular metal rings soldered on the PCB. The IC to the right is the ECL VCO, and the one to the left is the frequency divider.

3.3.3.1 Power Supply to the Sensor Probe

Looking into the datasheets of all the components used in this project, it is seen that the chosen components have different minimum and maximum supply voltage

limits. A voltage and current budget is made to consider different options for the power supply as shown in Fig. 3.11. Different alternatives were considered, before coming down to considering two options - to either use 2x1,5V batteries (3V) and a step-up voltage regulator, or to use 4x1,5V batteries (6V) and a step-down/Low-DropOut (LDO) voltage regulator. Since the pFET and the VCO have a minimum supply voltage of 3V and 4.2 V respectively, the first option is also eliminated. This leads to the second option being implemented, that is using a power supply of 6V and switching down the voltage to desired levels.

Since the components have different supply voltage requirements and all does not fit into one solution only, two step down/LDO voltage regulators are needed. One to switch down the supply voltage to 3V for the microcontroller, and one to switch down the voltage to 5V and use for all other components.

	6V	**5V**	**3V3**
	CD5051	LMT85	STM32WLE5JCI6TR
	555 timer	MC100EL1648	
	SN54HC4040	AP22815	
	LDO/Step up/down		
	alt. Digital temp		
	IC	**Supply Voltage**	**Power supply current (mA)**
p-FET	AP22815	3.0 - 5.0 V	0,0003
MUX	CD5051	0 - 20.0 V	0,000001
Temp. sensor	LMT85	1.8 - 5.5 V	0,005
VCO	MC100EL1648	4.2 - 5.5 V	0,019
Frequency divider	SN54HC4040	2 .0 - 6.0 V	0,00008
Oscillator	555 timer	2.0 - 16.0 V	0,00003
STM32WL55CCU7	cpu	1.8 - 3.6 V	0,005
3V3 LDO	LDO regulator	3.8 - 10 V	0,0000011
5V LDO	LDO regulator	5.5 - 45 V	0,0052
		All components:	Total supply current (mA):
		3V3 from LDO	34,6121
		5-5.5V from LDO	5,3
		6 V from battery	24,03
			5,2821

Figure 3.11: The components used in this project are listed together with their supply voltage limits, for a power supply voltage to be chosen for the sensor probe.

3.3.3.2 One Level of Sensors in the Probe

Each PCB has two MUXs used to control the signals to and from the sensors on one level in the probe. One sensor at a time is powered on, which is controlled by a power switch, pFET. The three sensors can therefore not be read at the same time. It is pre-determined by the microcontroller when each sensor is to be powered on by the MUX and the pFET and which sensor the microcontroller therefore can read from, but the three sensors are read very close in time, since the user should be able to know the data from the three sensors on each level approximately at the same time. Fig. 3.12 shows a block diagram of the setup of the sensors on the designed PCB, together with the DEMUX and MUX to control which sensor to power on and read from.

The PCB is designed in Altium Designer, with the dimensions 21 x 152 mm (width x length). It is divided into three sections, where the HFC sensor is to the far left of the PCB, the analog temperature sensor in the middle, and the capacitive sensor with the arc-shaped plates to the right. The PCB model with the three sensors, without the plates and the annular rings mounted, is shown in Fig. 3.13. The headers J1 and J2 to the far right in Fig. 3.13 are for the connections with the microcontroller and the power source, i.e the batteries. A total of nine pins are needed for the connections of the sensor probe with the power source and the microcontroller, but a 9-pin header was not found at the time of the search and two 6-pin headers are therefore used instead.

Three digital signals and one analog signal from the microcontroller are connected to the MUXs U5 and U6 in Fig. 3.13. A and B in Fig. 3.12 being the selector variables of the MUXs, *Digital IN* to enable DEMUX and *Utsignal* to read analog signal of the MUX. Two of the nine pins are for ground and voltage, and the last three pins, C1, C2 and C3, are three digital control pins to select one of three PCBs/levels (more about that in section 3.3.3.3).

3.3.3.3 Three Levels of Sensors

As can be seen already in the block diagram in Fig. 3.12, three digital pins C1, C2, C3 are added to the design. Since there is a total of nine sensors in one sensor probe, three sensors on each of three PCBs on the three different levels, and only one sensor can be read at a time, those three digital pins (C1-C3) are used to control which PCB (i.e. which level) to power on at a time. That is controlled by setting one of the three digital pins (C1-C3) to high (digital 1), and the other two pins to low (digital 0). Then one PCB is powered on at the time. Once one PCB (i.e. one level) has power, the three sensors on that PCB are supplied with power one at the time with

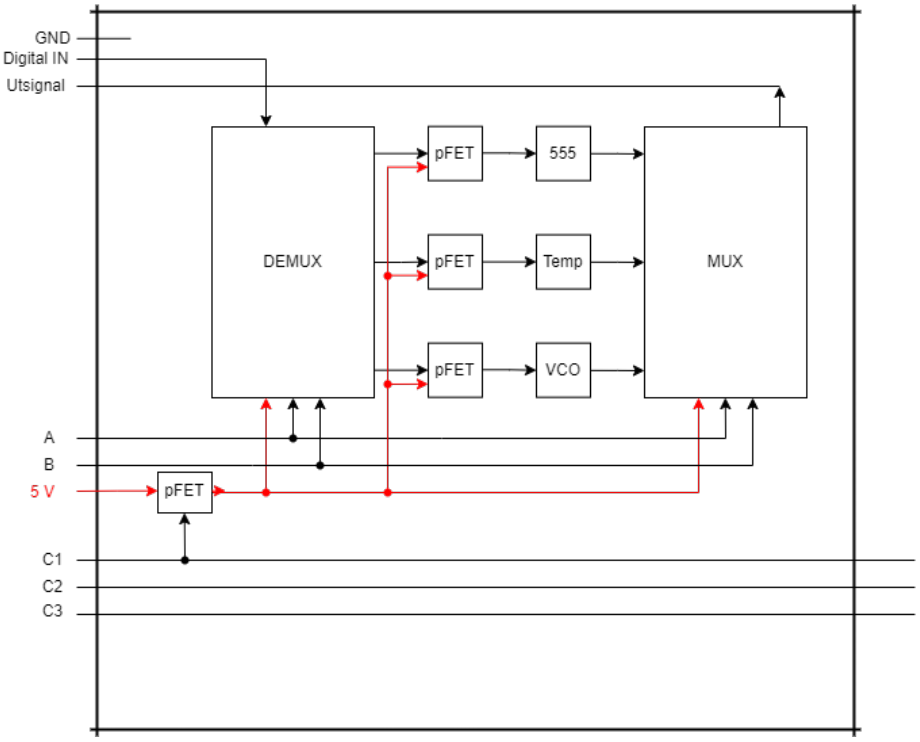

Figure 3.12: A block diagram illustrating the connections between the components on one level in the probe. To the far left, the input pins to the level are labeled. Digital IN is used to enable the DEMUX, Utsignal is to read the analog signal. The control pins A and B are used to choose a channel to write to or read from with the DEMUX/MUX. C1, C2, and C3 are control pins used to activate (power on) one PCB/one level at the time.

the help of the DEMUX to choose which sensor to power on and a pFET to switch on the power of the chosen sensor, to take measurements on that level. When the three measurements have been taken on one level (one at the time), power is switch off of that PCB and the next level is supplied with power to take measurements on that level, again with measurements taken from one sensor at the time.

The microcontroller and the sensor probe are configured so that the highest level, i.e. the level closet to the ground, is level number one. The second level is the middle level in the probe and the third level is the lowest level, i.e. the deepest level in the soil. The different levels are place approximately 20 cm from each other in the sensor probe. The sensors on each PCB are configured to be switched on in the following order - first the capacitive sensor with the arc-shaped plates, then the temperature

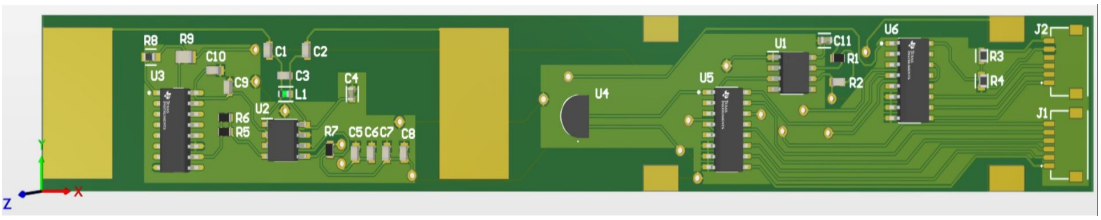

Figure 3.13: The PCB model designed in Altium Designer.

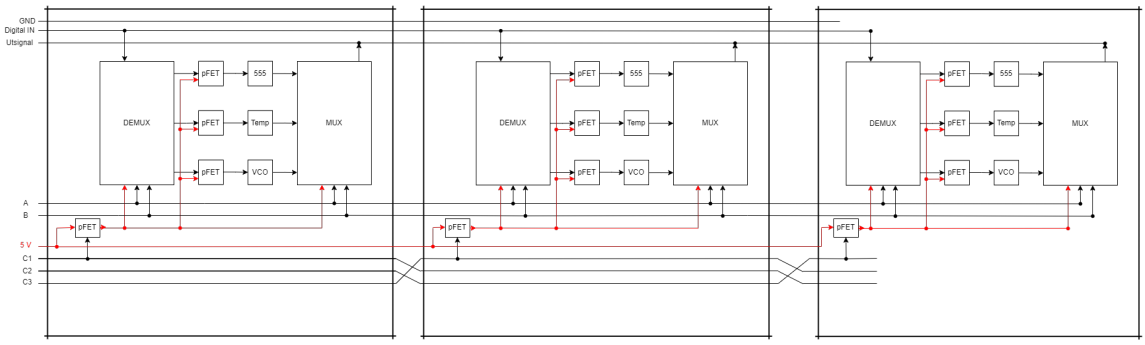

Figure 3.14: A block diagram illustrating the connections of the three levels of the sensor probe. Each level has its own PCB, with the three control pins C1-C3 rotating between the levels. One of the control pins is high at the time, while the other two are low, to power on one level at the time.

sensor, and after that the HFC sensor. Each sensor is switched on for two seconds, during which the measurements are taken, and then the sensor is switched off again. Five measurements are taken during these two seconds, and the average of those are then calculated and presented. One second is set initially as a delay between the different sensors being switched on. More about that can be read in section 5.

Chapter 4

Results and Discussion

Most of the tasks that needed to be completed to develop the first prototype of the multi-depth sensor probe were done. The two capacitive sensors were developed, together with the complete design of the sensor probe with both electronics and PCB design. The LoRa communication between the sensor probe and a gateway was not implemented due to delays in the project. Neither was the testing of multiple sensor probes on a large test-bed. There were challenges with getting a signal from the high frequency capacitive sensor with annular ring electrodes, and the development of that sensor exceeded the time plan. At last, after experimenting with different component values in the tank circuit, the wished frequency measurement was achieved.

Decisions have been taken during the project to try to minimize both costs and power consumption of one sensor probe, and to get a long lifetime. The total supply current needed for one sensor probe, as shown in Fig. 3.11, is used together with different duty cycles to calculate how often measurements can be taken to have as long life-time as possible. Different calculations are shown in Fig. 4.1. Based on the assumption of taking a total of one minute to power on all sensors and completing the measurements, and doing this every two hours, the batteries of one sensor probe will last a little more than four months. When instead increasing the number of measurements to once every 15 minutes, the sensor probe will only last for approximately 16 days.

Changing batteries several times a year is not easy to do in a sensing network with many probes. The wish is to have a longer lifetime to avoid the need of changing batteries often. Choosing other components together with considering the amount of measurements needed per day can help prolong the lifetime of one sensor probe. There might not be big changes in the soil every 15 minutes, and it might therefore be unnecessary to have that frequent measurements.

	Duty cycle	ON/period
1 min ON, 119 min OFF	0,83333333	%
1 min ON, 59 min OFF	1,66666667	%
1min ON, 29 min OFF	3,33333333	%
1 min ON, 19 min OFF	5	%
1 min ON, 14 min OFF	6,66666667	%
battery life = battery capacitance/total load current		
battery capacitance	2700	mAh
total current of probe	103,8363	mA
battery life =	26,0024673	h
With 0,833% duty cycle	0,86495638	mA
time = capacity/current	3121,5447	h
	130,064362	days
With 1,67% duty cycle	1,73406621	mA
time = capacity/current	1557,03397	h
	64,8764155	days
With 3,33% duty cycle	3,46121	mA
time = capacity/current	780,07402	h
	32,5030842	days
With 5% duty cycle	5,191815	mA
time = capacity/current	520,049347	h
	21,6687228	days
With 6,67% duty cycle	6,92242	mA
time = capacity/current	390,03701	h
	16,2515421	days

Figure 4.1: Using different duty cycles to calculate the life-span of one sensor probe.

4.1 Measurement Data

When doing some initial tests, only one sensor probe was tested and only to get one measurement from each sensor. To get more data, longer tests need to be made. Results from one test run, getting readings from each sensor on each level in the probe, are presented in Fig. 4.2. All measurements were made with the probe being surrounded by air, which explains why the data from the three levels are very close.

While testing the sensor probe, a human hand was wrapped around the sensors on one of the levels, and a decrease in the frequency could be observed. Since the human body contains a lot of water, the dielectric constant of the hand is higher than of water, which explains the decrease in frequency.

```
Measurement readings
Level 1:
Cap. sensor:  1.15 MHz
Temp. sensor:  23 C
HFC sensor:  130.63 MHz

Level 2:
Cap. sensor:  1.07 MHz
Temp. sensor:  22.6 C
HFC sensor:  133.70 MHz

Level 3:
Cap. sensor:  1.09 MHz
Temp. sensor:  22.8 C
HFC sensor:  132.70 MHz
```

Figure 4.2: Results from one test, where readings from each of the sensors in the probe are presented.

For the capacitive sensors, once the frequency is measured, the capacitance can be calculated. With the capacitance known, the dielectric constant can be calculated as well. From the dielectric constant, the moisture content can be evaluated. One thing to keep in mind when reading the results presented in Fig. 4.2, is that the frequency of the HFC sensor is first divided with a frequency divider, before it is sent to the microcontroller due to the high frequency. When presented, the measured frequency is multiplied with the divided number to get the actual frequency of the sensor. The reading from the temperature sensor is used together with Eq. (3.1) before it is presented.

Chapter 5

Conclusion and Future Work

5.1 Conclusion

The aim of this thesis project was to develop a sensor probe that can be industrialized at a low cost, and to do testings of the complete sensing system in a large test-bed. Due to challenges with the HFC sensor with annular electrodes, all parts of the project were not completed. The two capacitive sensors were implemented and testings of the sensors show that the frequency changes as it should, depending on the surrounding around the probe. The higher the dielectric constant of the surrounding is, the lower the frequency. The complete design of the electronics, the connections between the three levels and the PCB design were implemented as well. On the other hand, the communication between the sensor probe and a gateway still needs to be implemented, as well as the testing of the complete sensing system.

There have been challenges with this project, and the most challenging part was to get the HFC sensor running, and to implement the software in STM32IDE. It was challenging to find the right values of the components in the tank circuit of the HFC sensor, even though the datasheet of the VCO had an example. Since one of the capacitors in the example of the tank circuit was substituted with the electrodes of the capacitive sensor, the same values as the example could not be used and therefore needed further testings. The challenges with the STM32IDE was mainly the configuration of the different pins and the use of a timer to read the frequencies of the sensors, but there are good examples online that was followed and helped overcome the challenges.

To conclude, the achieved results show that longer lifetime of a sensor probe is needed, as well as further development, before the sensor probe can be industrialized.

5.2 Future

With this being a first prototype of a sensor probe, there are several things that can be improved, and there is still future work that needs to be done before this prototype can be industrialized.

One important parameter that can be improved is the measuring time. In this project, each sensor was switched on for two seconds, and one second of delay was used between the different sensors being switched on. This is a long unwanted time considering the fast processing time and the wish to have a real-time sensing system. Investigations can be made to get the necessary measuring time and to therefore shorten the total active time of a sensor probe.

The dimensions of the capacitive sensor plates were partly investigated in this project, where different lengths of the plates were tested to see if it had an impact on the frequency. The dimensions of the annular rings, on the other hand, can be further investigated. Different widths of the rings and distances between the rings can be tested to investigate if it has an impact on the measured frequency.

Another thing that might be able to be improved is the distance between the three sensors on a PCB. The distances between the three sensors were just randomly estimated, but investigations and calculations can be made to check if the sensors have an impact on each other and the performance, specially with the fringing field and the plates and rings of the capacitive sensors. If the sensors do not disturb each other, the PCB dimension can be shortened and material and costs can therefore be saved. If, on the other hand, the sensors do have an impact on each other, the distances must be increased to give more accurate measurements.

In this project four 1,5V AA batteries were used, which generated a total of approximately 6V. Since the VCO has a limit of maximum supply voltage of 5.5V, an LDO was needed to switch down the supply voltage to 5V, which causes energy losses and unwanted heat. One improvement can be to find a VCO that has a higher maximum supply voltage, so that all components can be supplied with 6V to avoid waste of energy, and heat problems.

The VCO used in the project, MC100EL1648, has a relatively high supply current. If this is changed to another VCO, not only energy losses are saved due to switching down the supply voltage, but the battery lives can also be prolonged. One example of a VCO that has very low current and power consumption is MAX2620. It can be worth investigating it further and trying to change MC100EL1648 to a MAX2620.

There are also still some future work that needs to be done. Testings with multiple sensor probes communicating with one gateway are needed, as well as testings in larger testbeds, with multiple sensor probes with larger distances. These kind of testings were originally part of this project, but due to some circumstances, time was not enough and this could therefore not be done.

Bibliography

[1] Asawa, G. L. *Irrigation and water resources Engineering.* New age international (P) limited, publishers, New Delhi, India, 2008.

[2] L. W. McKeen, "Chapter 2 - Introduction to the Properties of Plastic and Elastomer Films" www.sciencedirect.com. 2012. [Online]. Available: `https://www.sciencedirect.com/science/article/pii/B9781455725519000025` [Accessed: Jan. 30, 2023]

[3] Biomaker, "Capacitive Soil Moisture Sensor", Biomaker.org. Dec. 17, 2021. [Online]. Available: `https://www.biomaker.org/block-catalogue/2021/12/17/soil-moisture-sensor-aideepen-v12`. [Accessed: June. 19, 2023]

[4] L. Calderone, "Soil Moisture Sensors in Agriculture," Agritechtomorrow.com. Sept. 7, 2019. [Online]. Available: `https://www.agritechtomorrow.com/article/2019/07/soil-moisture-sensors-in-agriculture/11534`. [Accessed: Jan. 30, 2023]

[5] Tianming Chen, *Capacitive sensors for measuring complex permittivity of planar and cylindrical structures.* Iowa State University, 2012.

[6] Comsol, "Computing the Effect of Fringing Fields on Capacitance," Comsol.com. [Online]. Available: https://www.comsol.co.in/model/computing-the-effect-of-fringing-fields-on-capacitance-12605. [Accessed: Jan. 30, 2023]

[7] Zhenran Gao ID , Yan Zhu ID , Cheng Liu, Hongzhou Qian, Weixing Cao, Jun Ni, *Design and Test of a Soil Profile Moisture Sensor Based on Sensitive Soil Layers.* National Engineering and Technology Center for Information Agriculture, Published 21 May 2018.

[8] Developer Portal, "What are LoRa and LoRaWAN?," lora-developers.semtech.com. [Online]. Available: `https://lora-developers.semtech.com/documentation/tech-papers-and-guides/lora-and-lorawan/`

[9] Microtonics, “LoRa und 3G in einem Modul,” microtonics.com. Okt. 24, 2018. [Online]. Available: https://microtronics.com/blog/lora-und-2g-einem-modul/ [Accessed: Feb. 4, 2023]

[10] STMicroelectronics, “STM32WL55JC, Product Overview.” [Online]. Available: https://www.st.com/en/microcontrollers-microprocessors/stm32wl55jc.html [Accessed: Feb. 5, 2023]

[11] STMicroelectronics, ”Multiprotocol LPWAN dual core 32-bit Arm® Cortex®-M4/M0+ LoRa®, (G)FSK, (G)MSK, BPSK, up to 256KB Flash, 64KB SRAM,” STM32WL55xx Datasheet, Nov. 2020 [DS13293 Rev 1].

[12] Ettron, ”What is a 555 Timer IC — Using 555 Timer IC for Monostable Circuit,” ettron.com. [Online]. Available: https://ettron.com/what-is-a-555-timer-and-how-to-use-a-555-timer-ic/#:~:text=The%20two%20main%20versions%20of%20the%20555%20timer,within%20temperature%20of%200%20to%2070%20o%20C. [Accessed: Feb. 5, 2023]

[13] Texas Instruments, “LMC555 CMOS Timer” LMC555 datasheet, Feb. 2020 [Revised July. 2016].

[14] R.N. Mutagi, ”Use Emitter Coupled Logic in your RF Applications,” *RF featured technology*, pp. 26-32, April 1994. [Online]. Available: https://www.researchgate.net/publication/230813084_Use_Emitter_Coupled_Logic_in_your_RF_Applications

[15] ON Semiconducter, ”5 V ECL Voltage Controlled Oscillator Amplifier,” MC100EL1648 datasheet, 2008. [Revised March, 2021].

[16] Texas Instruments, ”LMT85 1.8-V, SC70/TO-92/TO-92S, Analog Temperature Sensors,” LMT85 datasheet, March. 2013 [Revised Oct. 2017].

[17] Texas Instruments, ”CD405xB CMOS Single 8-Channel Analog Multiplexer or Demultiplexer With Logic-Level Conversion,” CD4052B datasheet, Aug. 1998. [Revised March. 2023].

[18] Educba, ”What is IDE?,” educba.com. [Online]. Available: https://www.educba.com/what-is-ide/ [Accessed: Feb. 11, 2023]

[19] STMicroelectronics, ”STM32CubeIDE Integrated Development Environment for STM32,” st.com. [Online]. Available: https://www.st.com/en/development-tools/stm32cubeide.html [Accessed: Feb. 11, 2023]

[20] STMicroelectronics, "Integrated development environment for STM32 products," st.com. [Online]. Available: https://www.st.com/resource/en/data_brief/stm32cubeide.pdf [Accessed: Feb. 11, 2023]